SUPPORTING INFORMATION

Isokinetic Temperature and Size-Controlled Activation of Ruthenium-Catalyzed Ammonia Borane Hydrolysis

Hanyu Ma and Chongzheng Na*

[1]Department of Civil and Environmental Engineering and Earth Sciences,

University of Notre Dame, Notre Dame, IN 46556, USA

*Corresponding Author: chongzheng.na@gmail.com.

Table S1. Literature Data Used to Plot Figure 1

Catalyst	diameter (nm)	ln*A* (mol-H_2 m^{-2}-catalyst h^{-1})	E_a (kJ mol^{-1})	Reference
Ru	2.2	8.3	27.5	17
Ru	1.9	21.0	54.0	18
Ru	2.6	17.5	47.0	19
Ru	1.7	13.9	34.8	20
Ru	2.9	33.8	33.0	21
Ru	2.5	13.3	48.0	16
Ru	2.5	17.3	11.7	22
Ru	1.2	2.8	38.2	23
Ru	2.0	14.7	70.0	24
Ru	2.3	27.9	77.0	25
Ru	4.4	30.8	58.0	26
Ru	4.7	23.2	34.8	27
Pt	1.3	18.8	47.7	28
Pt	1.5	8.8	24.3	29
Pd	3.5	15.2	44.0	18
Pd	1.41	9.1	32.5	30
Pd	4	17.0	51.0	31
Pd	4	14.0	40.0	32
Pd	6	21.5	52.0	33
Ni	3.2	8.1	28.0	34
Ni	3.2	11.0	34.0	35
Ni	10.0	9.3	31.6	36
Co	2.6	9.5	28.2	37
Co	3.2	16.4	50.0	38
Co	2.3	21.9	62.0	39
Co	7.2	15.6	46.0	40
Fe	6.3	12.1	37.0	41

Table S2. Selection of Data for Performing the Linear Regression in Figure 4a

Number of Data†	k_0 (mmol-H_2 min^{-1})	Decrease of k_0 (mmol-H_2 min^{-1})	Does the decrease of k_0 exceed its standard error?‡
3	0.367(±0.012)		N/A
5	0.359(±0.014)	0.008	No
7	0.351(±0.008)	0.008	No
9	0.330(±0.009)	0.021	Yes
11	0.309(±0.010)	0.021	Yes

† Data included in each regression are selected around the middle point with a molar accumulation of hydrogen production, *n*, close to the average of all data presented in Figure 4a. According to the interpretation of the reaction regimes (i.e., I: Ru^0 formation; II: stable reduction of NH_3BH_3; and III: NH_3BH_3 depletion), the reaction rate associated with the middle point is most representative of the reaction kinetics of Regime II, providing the estimate of k_0 of our interest. To minimize the influence of random errors from measurements, we perform linear regression involving the data points on both sides of the middle point. For example, a 3-point regression involves 1 point with *n* greater than that of the middle point and 1 point with *n* smaller than the middle *n*.

‡ The random errors conforming to a normal distribution should not cause the estimate of k_0 to deviate too much from its true value. In comparison, the inclusion of data from Regimes I and III would cause dramatic change of the slope of the linearity and thus the estimate of k_0. This criterion is used to determine how many data points around the middle point are included in the regression and examined by comparing the decrease of k_0 with the standard errors of k_0, as listed in the parentheses of the second column. For the data presented in Figure 4a, 7 data points are used to estimate k_0 for further analyses.

Table S3. Reduction in Catalytic Activity of Supported Ru Nanoparticles Reported in the Literature

Catalyst	Number of Runs	TOF/TOF_0 (%)	Reference
Ru on hydroxyapatite	5	92	27
Ru on zeolite	5	85	67
Ru@Ni on graphene	5	78	65
Ru on graphene	4	72 (~64 after 5^{th} run)	23
Ru@Co on graphene	5	51	66
Ru on carbon black	5	42	20
Ru on multi-walled carbon nanotubes	4	41 (~27 after 5^{th} run)	16

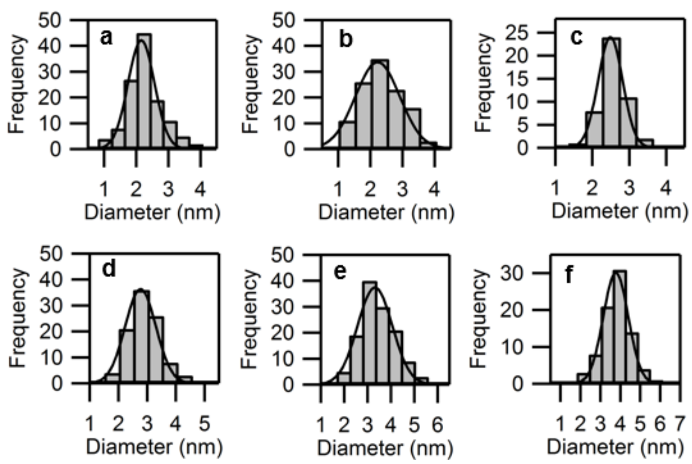

Figure S1. Histograms of the nominal diameters of Ru-FCC nanoparticles supported on layered double oxide nanodiscs. Percentage of Ru in each sample: *a*, 1.1%; *b*, 2.6%; *c*, 3.0%; *d*, 3.2%; *e*, 4.5%; *f*, 8.8%.

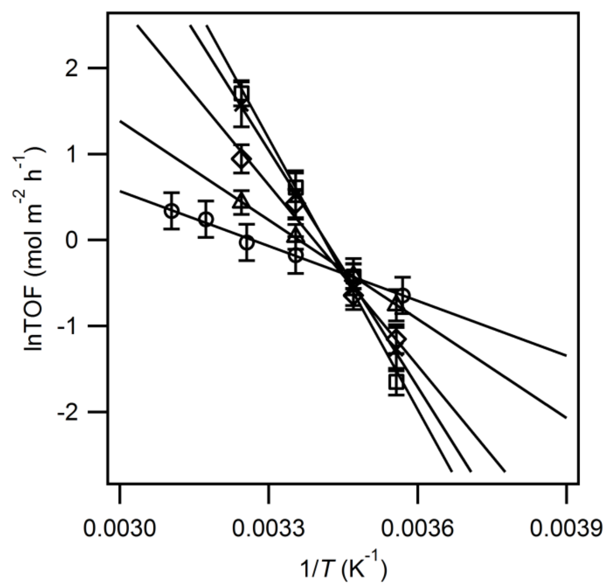

Figure S2. Correlation of the turnover frequency (TOF) with temperature *T* for Ru-FCC with five different sizes. Ru-FCC with different diameters are represented by different symbols: circle, 2.0(±0.4) nm; triangle, 2.4(±0.3) nm; rhombus, 2.7(±0.5) nm; cross, 3.2(±0.8) nm; square, 3.8(±0.5) nm. Lines crossing at the isokinetic temperature are obtained by regression according to the Arrhenius equation (Equation 1).

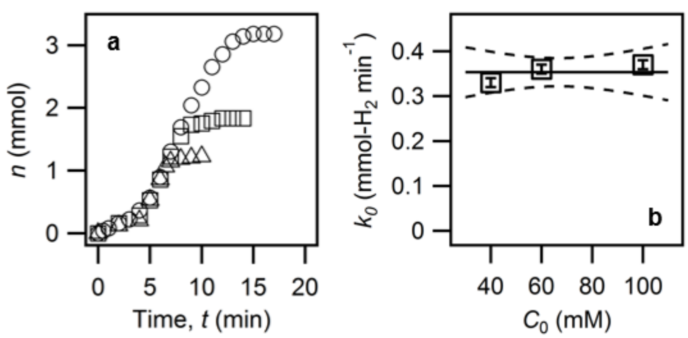

Figure S3. Independence of ammonia borane hydrolysis on the initial concentration C_0. (a) Accumulation of the number of moles of hydrogen generated by hydrolysis, n, over time t, which is used to estimate the pseudo-zeroth order rate constant k_0 (circles, C_0 = 100 mM; squares, C_0 = 60 mM; triangles, C_0 = 40 mM). (b) Invariance of k_0 with C_0. Solid and dashed curves represent the average and 95% confidence bands. Error bars represent standard errors. Mean diameter of Ru-FCC nanoparticles: 2 nm.

Note S1. Fraction of Atoms Located at Edges and Corners in a Truncated Octahedron

The truncated octahedron has 14 facets including 8 {111} facets and 6 {100} ones with 24 edges and 12 corners. We denote l as the same length of each edge and $\phi = 0.262$ nm (see Figure 3b and the accompanying text) as the diameter of a ruthenium (Ru) atom. To derive the fraction, we first count the number of non-edge/corner atoms for the 14 facets. For the {111} facets, the number is:

$$N_{111} = 8 \times \frac{1}{2}\left(\frac{l}{\phi} - 3 + 1\right)\left(\frac{l}{\phi} - 3\right) = 4\left(\frac{l}{\phi} - 2\right)\left(\frac{l}{\phi} - 3\right) \qquad \text{(S1).}$$

For each {100} facets, the number of non-edge/corner atoms is:

$$N_{100} = 6\left(\frac{l}{\phi} - 2\right)^2 \qquad \text{(S2).}$$

Second, we count the number of non-corner atoms on the edges. For the 24 edges, we have:

$$N_e = 24\left(\frac{l}{\phi} - 2\right) \qquad \text{(S3).}$$

Third, we count the total number of corner atoms, which is

$$N_c = 12 \qquad \text{(S4).}$$

Since the nominal diameter d is the diagonal of the square {100} facet:

$$d = \sqrt{2}\,(l - \phi) + \phi = \sqrt{2}l - \left(\sqrt{2} - 1\right)\phi \qquad \text{(S5).}$$

So

$$l = \frac{d}{\sqrt{2}} + \left(1 - \frac{1}{\sqrt{2}}\right)\phi \qquad \text{(S6).}$$

Since

$$f = \frac{N_e + N_c}{N_{111} + N_{100} + N_e + N_c} \qquad \text{(S7),}$$

combining Equation S7 with Equations S1 – S4 and S6 gives:

$$f = \frac{12\left[\sqrt{2}d\phi - \left(\sqrt{2} + 1\right)\phi^2\right]}{5d^2 - 10d\phi + 7\phi^2} \qquad \text{(S8),}$$

With $\phi = 0.262$ nm and d in nanometers, we have:

$$f = \frac{0.89d - 0.40}{d^2 - 0.52d + 0.096} \qquad \text{(21).}$$